

# Thermochronology and the three-dimensional cooling pattern of a granitic pluton: an example from the Toki granite, Central Japan

Takashi Yuguchi · Kenji Amano · Tadahiko Tsuruta · Tohru Danhara · Tadao Nishiyama

Received: 10 November 2010 / Accepted: 9 April 2011 / Published online: 28 April 2011  
© Springer-Verlag 2011

**Abstract** The three-dimensional spatial variations in the cooling pattern of the Toki granitic body, a zoned pluton in Central Japan, have been evaluated quantitatively by thermochronology using cooling age determination based on the different closure temperatures for target mineral species. The Toki granite has hornblende K–Ar ages of about  $74.3 \pm 3.7$  Ma ( $N = 2$ ; closure temperature of  $510 \pm 25^\circ\text{C}$ ), biotite K–Ar ages of  $78.5 \pm 3.9$  to  $59.7 \pm 1.5$  Ma ( $N = 33$ ;  $300 \pm 50^\circ\text{C}$ ), and zircon fission-track ages of  $75.6 \pm 3.3$  to  $52.8 \pm 2.6$  Ma ( $N = 44$ ;  $240 \pm 50^\circ\text{C}$ ). The spatial variation in the biotite K–Ar age is similar to that in the zircon fission-track age in samples collected from 11 boreholes and seven outcrop sites in the Toki granite, indicating that cooling was effectively from

the roof and also from the northwest margin. This cooling pattern shows a strong correlation with the Alumina Saturation Index (ASI) distribution of the body. Larger ASI values correspond to earlier and more rapid cooling after emplacement and smaller value to slower cooling. Toki granite was effectively cooled from the peraluminous regions where assimilation of country sedimentary rock was most extensive.

**Keywords** Cooling process · Granitic pluton · Thermochronology · K–Ar dating · Fission-track dating · Toki granite

Communicated by J. Blundy.

T. Yuguchi (✉) · T. Tsuruta  
Mizunami Underground Research Laboratory, Geological Isolation Research and Development Directorate, Japan Atomic Energy Agency, 1-64, Yamanouchi, Akeyo, Mizunami, Gifu 509-6132, Japan  
e-mail: yuguchi.takashi@jaea.go.jp

K. Amano  
Horonobe Underground Research Center, Geological Isolation Research and Development Directorate, Japan Atomic Energy Agency, 1-8, Miyazono, Horonobe, Teshio, Hokkaido 098-3207, Japan

T. Tsuruta · T. Nishiyama  
Department of Earth and Environmental Sciences, School of Science, Graduate School of Science and Technology, Kumamoto University, 2-39-1, Kurokami, Kumamoto 860-8555, Japan

T. Danhara  
Kyoto Fission-Track Co., Ltd, 44-4, Minamitajiri, Omiya, Kita-ku, Kyoto 603-8832, Japan

## Introduction

Thermochronology, which is based on multiple dating methods utilizing different closure temperatures for target minerals, is a powerful tool for quantifying a cooling process of a granitic body. The cooling process such as direction of heat release and the cooling rate will give important information about the size and configuration of the pluton in the crust and also about the depth of the intrusion, some of which can be evaluated independently by geological and petrological methods. Knowledge of the cooling also has potential practical application in understanding the distribution of fractures (e.g., cooling joints) and the hydrothermal circulation in a pluton.

The application of thermochronometry to one particular sample (i.e., one particular position) inside the granite can clarify the “sub-solidus temperature–time path” that the plutonic rock has undergone. Additionally, the application of thermochronology to multiple samples widely collected from a granite, i.e., “multi-sampling thermochronology,” can reveal the three-dimensional cooling pattern of a pluton

through the spatiotemporal change of temperature inside the body. There has been a lot of discussion about cooling rate and uplift history of granitic bodies based on thermochronology (e.g., Dodson and McClelland-Brown 1985; Hurford 1986; Yuhara and Kagami 1995; Tsuchiya and Fujino 2000; Umeda et al. 2001; Zhao et al. 2004). However, there have been few attempts to clarify the three-dimensional cooling pattern of an individual pluton. Only a few studies based on “multi-sampling thermochronology” investigated vertical (e.g., Harayama 1992, 1994; Eby et al. 1995) or horizontal variations (e.g., Bando et al. 2003; Oikawa et al. 2006) of the cooling process. Harayama (1992, 1994) described vertical variations in cooling rate of the Plio-Pleistocene Takidani Granodiorite, Central Japan. He showed that there was a difference in the cooling rate between higher and lower levels in the granodiorite based on biotite, K-feldspar and hornblende K–Ar dating, and zircon fission-track dating for four samples collected from various levels. Oikawa et al. (2006) described the horizontal variations in the cooling pattern of the Miocene Ichifusayama Granodiorite, Kyushu, Japan. They suggested an unusual manner of cooling such that the rate of cooling from 300 to 100°C in the central part of the body was about 100°C/m.y., i.e., faster than that in the periphery, based on biotite K–Ar, zircon fission-track, and apatite fission-track dating for four samples. Oikawa et al. (2006) concluded that the influence of paleotopography resulted in the anomalous cooling pattern inside the body.

This study investigated the three-dimensional cooling pattern in a granitic body, the Toki granite, Central Japan (Fig. 1), by employing “multi-sampling thermochronology.” The Toki granite is a good example for such a study because the petrography was already described by Yuguchi et al. (2010) and the rock mass is clarified to have solidified as a zoned pluton of Late Cretaceous age. Nineteen boreholes were drilled in the Toki granite (Fig. 2a) by Japan Atomic Energy Agency (JAEA) for the “Regional Hydrological Study (Japan Nuclear Cycle Development Institute 2000)” and for the “Mizunami Underground Research Laboratory Project (Japan Nuclear Cycle Development Institute 2002).” The borehole lengths range from about 500 m to 1,300 m. Samples collected from 11 boreholes and seven outcrops in the Toki granite display spatial variations in mineral ages within the body in three dimensions (Fig. 2a), which can be related to difference in cooling rate of the magmatic body. Availability of these samples allows placing accurate constraints on the three-dimensional cooling process of the Toki granite using “multi-sampling thermochronology.”

Good indicators of low-temperature closure thermochronometry in granite include biotite K–Ar dating and zircon fission-track dating. The data are mapped according to horizontal location and vertical elevation within the body.

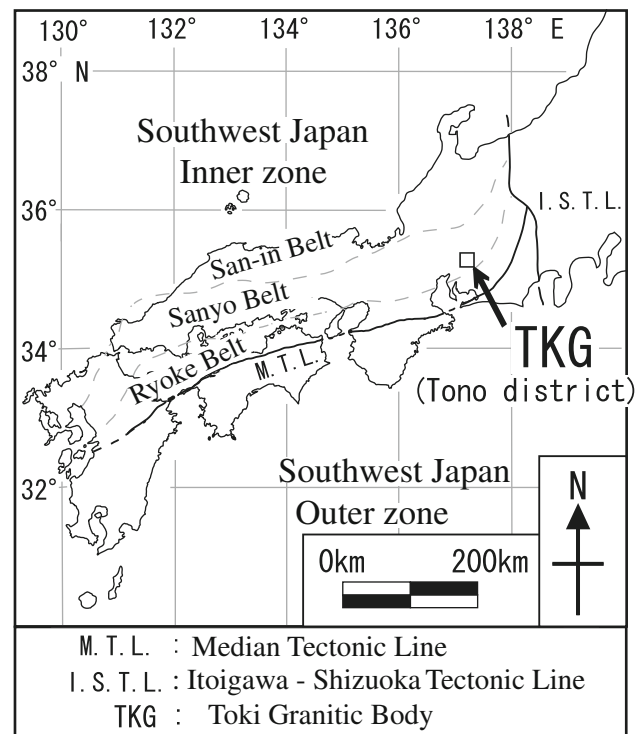


**Fig. 1** Location map showing the Toki granite (Tono district; square symbol) in Central Japan, together with the distribution of San-in, Sanyo and Ryoke Belts in the Inner Zone of Southwest Japan, after Ishihara and Chappell (2007)

The cooling patterns of the Toki granite at the temperature of biotite K–Ar closure ( $300 \pm 50^\circ\text{C}$ ) and zircon fission-track closure ( $240 \pm 50^\circ\text{C}$ ) stages, respectively, are evaluated based on the spatial variations in the data.

### The Toki granite

The southwest Japan is divided by the Median Tectonic Line (M.T.L.) into Inner and Outer Zones (Fig. 1). Igneous rocks of Cretaceous to Palaeogene age in the Inner Zone of Southwest Japan occur in the parallel, northeast–southwest oriented Ryoke, Sanyo and San-in Belts (Ishihara 2003). The Toki granite in the Tono district, Gifu, Central Japan, is one of the Late Cretaceous plutonic bodies of the Sanyo Belt (Ishihara and Chappell 2007; Fig. 1) and has been dated at  $68.3 \pm 1.8$  Ma (monazite chemical Th–U–total Pb isochron method (CHIME): Suzuki and Adachi 1998) and  $72.3 \pm 3.9$  Ma (whole-rock Rb–Sr: Shibata and Ishihara 1979).

The Toki granite is a nearly circular stock, with  $14 \times 12$  km<sup>2</sup> in areal extent (Yamada et al. 1990) and vertical thickness of at least 1.5 km based on borehole investigation. The Toki granite intruded into Jurassic sedimentary rocks (the Kamiasou Unit) of the Mino Terrane (Sano et al. 1992) and into the Nohi Rhyolite ( $85 \pm 5$  Ma

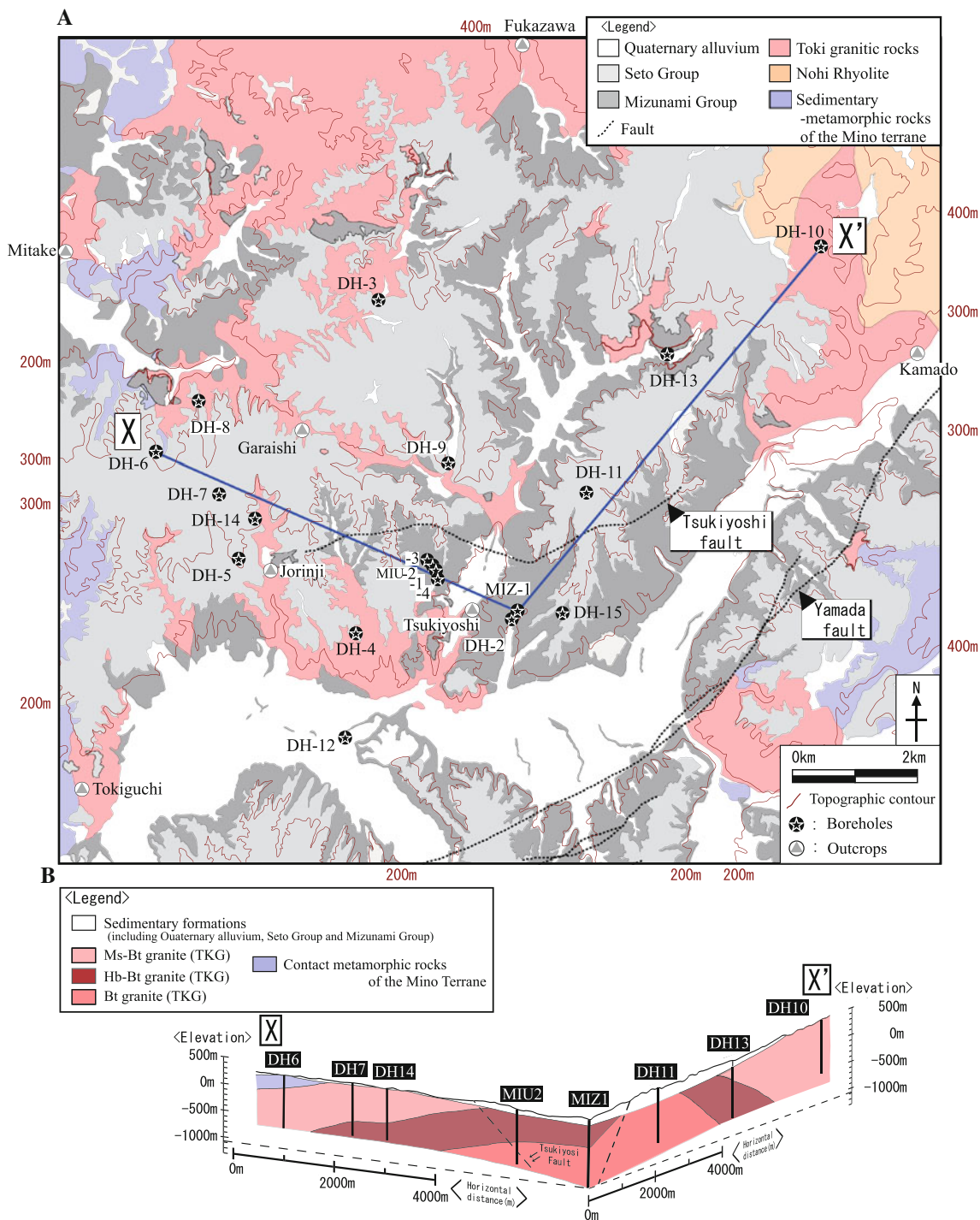


**Fig. 2** The Toki granitic pluton. **a** Geological map of the Tono district showing the Toki granite, after Itoigawa (1980), and borehole and outcrop sites in this study. The topographic contour inside the Tono district is based on Geographical Survey Institute, 1:25,000 topographic maps entitled Ontake, Takenami, Toki, and Mizunami.

**b** Rock facies cross-section for the Toki granite along the line from X to X' in the topography map (a); Ms-Bt granite, Muscovite-biotite granite; Hb-Bt granite, hornblende-biotite granite; Bt granite, biotite granite (Yuguchi et al. 2010)

of allanite CHIME; Suzuki et al. 1998; Fig. 2a). The Toki granite is surrounded by the sedimentary rocks of the Mino Terrane on the north and west and the Sumikawa granite on the south and the Nohi Rhyolite on the east (Yamashita

et al. 1988). The intrusive contacts between the Toki granite and the sedimentary rocks of the Mino Terrane are sharp and observed at an outcrop (N69°W 65°S) about 1 km north of the study area (Asia Air Survey 1997) and

also in a borehole DH-6 (N38°W 44°E at the elevation of 52.3 m). The pelitic and psammitic rocks of the Mino Terrane were metamorphosed to hornfels by the Toki granitic magma (Yamashita et al. 1988). The Toki granite is overlain unconformably by the Miocene Mizunami Group and the Pliocene Seto Group (Itoigawa 1974, 1980). The Toki granite and the Mizunami Group are cut by the Tsukiyoshi fault, a reverse, dip-slip fault with an approximate N80°W strike and 65–75°S dip (Yamashita et al. 1988; Ota et al. 1999). The Tsukiyoshi fault has been active intermittently since its formation in the Miocene up to the formation of Pliocene Seto Group (Fujii 2000).

The Toki granite is characterized by systematic spatial changes in rock facies (mode and mineral assemblage) and corresponding change in bulk chemical compositions and is interpreted to be a zoned pluton (Yuguchi et al. 2010). The rock facies grades from muscovite-biotite granite (MBG) at the margin through hornblende-biotite granite (HBG) to biotite granite (BG) in the interior (Fig. 2b). The boundaries of three rock facies are defined by the appearance (MBG/HBG) and disappearance (HBG/BG) of hornblende without accompanying chilled margin. The systematic change in the Alumina Saturation Index (ASI) values (mol.  $\text{Al}_2\text{O}_3/(\text{CaO} + \text{Na}_2\text{O} + \text{K}_2\text{O})$ ) from the MBG through HBG to BG corresponds to a systematic variation in the bulk chemistry from peraluminous at the margin to metaluminous in the interior. The  $\text{Fe}^{3+}/\text{Fe}^{2+}$  ratios gradually increase from MBG through HBG to BG, corresponding to a systematic change from ilmenite-series at the margin to magnetite-series in the interior (Yuguchi et al. 2010). This study employed hornblende, biotite, and zircon for the thermochronometry. Hornblende only occurs in the HBG, whereas biotite and zircon commonly occur throughout the Toki granite.

### Samples and analytical procedures

Samples used for this study were collected from 11 boreholes and seven outcrops (Fig. 2a) in order to examine the spatial variation in mineral ages in the cooling magma chamber. Hornblende, biotite, and zircon were separated from rock samples by a combination of grain size separation, magnetic separation using a Franz isodynamic separator, and density separation using conventional heavy liquid. Their representative compositions are listed in Table 1. Two data are obtained for hornblende K–Ar age, 33 data for biotite K–Ar age, and 44 data for zircon fission-track age (Tables 2, 3, 4).

The potassium and argon analyses were carried out at the Hiruzen Institute for Geology and Chronology Co. Ltd, Geospace Science Co. Ltd and Allegheny Technologies Japan Co. Ltd. Radiogenic argon concentrations were

analyzed with an isotope dilution mass spectrometer (Kratos MS-10S and AEI MS-10) following the technique of Dalrymple and Lanphere (1969). Potassium was determined with a flame emission spectrophotometry utilizing an internal standard. The isotopic ages of the samples were calculated using the standard K–Ar age equation (Dalrymple and Lanphere 1969; Dalrymple et al. 1999) with  $\lambda_e = 0.581 \times 10^{-10}/\text{year}$ ,  $\lambda_\beta = 4.962 \times 10^{-10}/\text{year}$  and  $^{40}\text{K}/\text{K} = 0.0001167$  of Steiger and Jäger (1977). The analytical uncertainties associated with the age determination were calculated using the method of Cox and Dalrymple (1967). K–Ar closure temperatures in this study are based on Dodson and McClelland-Brown (1985) as follows:  $510 \pm 25^\circ\text{C}$  for hornblende and  $300 \pm 50^\circ\text{C}$  for biotite.

Fission-track dating was carried out at Kyoto Fission-Track Co. Ltd, using zeta calibration method based on recommendation by the I.U.G.S. Subcommittee on Geochronology (Hurford 1900a, b). The density of spontaneous fission-tracks generated by  $^{238}\text{U}$  decay in a mineral is proportional to the age and the  $^{238}\text{U}$  content of the sample. The fission-track age are obtained by the following equation:

$$T = \frac{1}{\lambda_D} \ln \left( 1 + \lambda_D \cdot g \cdot \zeta \cdot \frac{\rho_s}{\rho_i} \cdot \rho_d \right)$$

where  $T$  = age,  $\lambda_D$  = total decay constant of  $^{238}\text{U}$ ,  $g$  = geometry factor depending on detector type (Gleadow and Lovering 1977),  $\zeta$  = zeta calibration factor,  $\rho_s/\rho_i$  = spontaneous/induced fission-track density ratio in the sample, and  $\rho_d$  = density of induced fission-track measured on the detector place in intimate contact with the glass monitor. Zircon samples were analyzed by the external detector method (ED1, internal mineral surface) using the geometry factor of 0.5 (Gleadow 1981). Zircons were etched in a NaOH and KOH eutectic mixture (Gleadow et al. 1976). Thermal irradiations of samples were carried out in the Rotary Specimen Rack of the TRIGA MARK II reactor at Rikkyo University and in the PN site of the JRR-4 reactor of JAEA. Fission-track ages were determined based on the zeta calibration approach described by Hurford and Green (1983). The total decay constant of  $^{238}\text{U}$  is  $\lambda_D = 1.55125 \times 10^{-10}/\text{year}$  (Steiger and Jäger 1977). Zeta calibration factors of zircon for ED1 are  $\zeta_{\text{ED1}} = 352 \pm 3$  (Danbara and Iwano 1983) for Rikkyo University reactor and  $\zeta_{\text{ED1}} = 380 \pm 3$  (Danbara et al. 2003) for JRR-4 reactor. The errors in zeta values are given to one sigma. Closure temperature for zircon fission-track dating is  $240 \pm 50^\circ\text{C}$  based on Dodson and McClelland-Brown (1985).

Characterization of zircon fission-track length measurements was also carried out for nine samples to test possible rejuvenation by massive reheating during the

**Table 1** Representative analyses of hornblende, biotite, and zircon from the Toki granite

Mineral	Hb	Hb	Bt	Bt	Zr	Zr
Sample no.	DH13-15	DH13-15	MIU2-34	MIU2-34	MIU2-13	MIZ1-23
Elevation	–216.00 m	–216.00 m	–496.72 m	–496.72 m	–85.72 m	–1,010.29 m
Location	03-core	03-rim	04-core	04-rim	02-core	03-core
<i>(wt%)</i>						
SiO <sub>2</sub>	39.16	40.01	33.90	33.97	32.70	31.76
TiO <sub>2</sub>	0.61	1.11	3.89	3.20	–	–
Al <sub>2</sub> O <sub>3</sub>	9.91	9.20	14.65	14.66	–	–
FeO	27.69	28.03	29.20	29.01	–	–
MnO	1.90	1.77	1.04	1.01	–	–
MgO	2.83	3.04	3.86	3.71	–	–
CaO	10.31	10.30	–	–	–	–
Na <sub>2</sub> O	1.95	1.90	0.42	0.45	–	–
K <sub>2</sub> O	1.15	0.96	9.63	10.11	–	–
ZrO <sub>2</sub>	–	–	–	–	64.40	58.04
HfO <sub>2</sub>	–	–	–	–	1.32	2.21
P <sub>2</sub> O <sub>5</sub>	–	–	–	–	–	1.91
ThO <sub>2</sub>	–	–	–	–	–	2.07
UO <sub>3</sub>	–	–	–	–	0.87	2.53
Total	95.51	96.32	96.59	96.12	99.29	98.52
<i>(atm)</i>						
O	23	23	22	22	4	4
Si	6.46	6.53	5.44	5.49	1.00	0.99
Ti	0.08	0.14	0.47	0.39	–	–
Al	1.93	1.77	2.77	2.79	–	–
Fe	3.82	3.83	3.92	3.92	–	–
Mn	0.27	0.24	0.14	0.14	–	–
Mg	0.70	0.74	0.92	0.89	–	–
Ca	1.82	1.80	–	–	–	–
Na	0.62	0.60	0.13	0.14	–	–
K	0.24	0.20	1.97	2.08	–	–
Zr	–	–	–	–	0.97	0.88
Hf	–	–	–	–	0.01	0.02
P	–	–	–	–	–	0.05
Th	–	–	–	–	–	0.01
U	–	–	–	–	0.01	0.02
Total	15.94	15.85	15.76	15.84	1.99	1.98

**Table 2** Hornblende K–Ar dating results from the Toki Granite

Sample description		Rock facies <sup>a</sup>	Sample location and elevation			K (wt%)	Rad. <sup>40</sup> Ar	Age (Ma) ± 1σ		
Borehole (B)/ outcrop (O)	Sample name		X (northing)	Y (easting)	Elevation (m)		(scc/gm × 10 <sup>–5</sup> )	(wt%)		
O	Mitake	KA-5Hbg	MBG	–63,940.0	350.0	290.0	1.25	0.37	73.6	74.6 ± 3.7
O	Mitake	KA-5Hby	MBG	–63,940.0	350.0	290.0	0.82	0.24	67.5	73.9 ± 3.7

<sup>a</sup> Rock facies of the Toki granite includes muscovite-biotite granite (MBG), hornblende-biotite granite (HBG), and biotite granite (BG)

cooling process, which were collected from three boreholes of DH-2, 10 and MIZ-1. Annealing will shorten the fission-track length, thus yielding a decrease in fission-track

density. Track length measurement (track number, mean, maximum and minimum length, standard deviation, and standard error) gives quantification of the shortening and

**Table 3** Biotite K–Ar dating results from the Toki Granite

Sample description		Rock facies <sup>a</sup>	Sample location and elevation			K (wt%)	Rad. <sup>40</sup> Ar ( $\text{scc/gm} \times 10^{-5}$ )	Age (Ma) $\pm 1\sigma$		
Borehole (B)/ outcrop (O)	Sample name		X (northing)	Y (easting)	Elevation (m)					
B	DH-2	DH02RA01	HBG	−69,125.0	6,437.4	−185.0	7.18	2.06	96.2	72.3 $\pm$ 1.8
B	DH-2	DH02RA03	BG	−69,125.0	6,437.4	−302.1	7.10	2.06	94.7	73.0 $\pm$ 1.8
B	DH-3	DH3-1	MBG	−64,489.2	4,416.3	77.0	6.24	1.86	92.2	75.0 $\pm$ 1.9
B	DH-3	DH3-2	MBG	−64,489.2	4,416.3	−479.7	5.80	1.68	89.2	73.1 $\pm$ 1.8
B	DH-8	FT-5	MBG	−66,002.9	1,871.9	47.3	5.87	1.69	98.2	72.9 $\pm$ 1.8
B	DH-8	FT-6	MBG	−66,002.9	1,871.9	−88.2	6.57	1.87	96.8	71.8 $\pm$ 1.6
B	DH-8	FT-7	MBG	−66,002.9	1,871.9	−439.6	6.37	1.84	98.4	73.0 $\pm$ 1.6
B	DH-8	FT-8a	MBG	−66,002.9	1,871.9	−610.7	6.46	1.86	98.4	72.9 $\pm$ 1.7
B	DH-8	FT-8b	MBG	−66,002.9	1,871.9	−739.7	6.44	1.86	98.4	72.9 $\pm$ 1.7
B	DH-10	DH10	MBG	−63,745.2	10,945.7	196.2	6.95	2.04	95.3	74.0 $\pm$ 1.8
B	DH-10	DH10RA	MBG	−63,745.2	10,945.7	−256.2	6.86	1.96	94.7	72.0 $\pm$ 1.8
B	DH-11	DH11-1	BG	−67,285.4	7,560.5	−116.7	2.62	0.69	88.6	66.3 $\pm$ 1.7
B	DH-11	DH11-2	BG	−67,285.4	7,560.5	−411.9	6.35	1.82	94.4	72.3 $\pm$ 1.8
B	DH-12	DH12	MBG	−70,695.4	3,935.0	−246.7	6.98	2.07	95.6	74.5 $\pm$ 1.9
B	DH-13	DH13	HBG	−65,324.7	8,625.8	−77.0	6.22	1.83	95.3	73.9 $\pm$ 1.8
B	MIU-1	KA-1bi	HBG	−68,280.3	5,217.4	108.6	4.64	1.37	90.7	74.1 $\pm$ 3.7
B	MIU-1	KA-2Bi	HBG	−68,280.3	5,217.4	−261.9	6.74	2.02	95.3	75.0 $\pm$ 3.8
B	MIU-1	KA-3Bi	BG	−68,280.3	5,217.4	−360.9	6.61	1.97	89.6	74.9 $\pm$ 3.7
B	MIU-1	KA-4Bi	BG	−68,280.3	5,217.4	−520.1	6.28	1.84	90.6	73.6 $\pm$ 3.7
B	MIU-4	MIU-4FT2-02	HBG	−68,292.5	5,353.0	−98.5	2.27	0.54	51.9	60.1 $\pm$ 1.5
B	MIU-4	MIU-4FT3-02	HBG	−68,268.7	5,376.7	−176.2	1.34	0.33	73.0	63.1 $\pm$ 1.6
B	MIU-4	MIU-4FT5-02	HBG	−68,237.2	5,408.2	−279.3	1.20	0.28	60.8	59.7 $\pm$ 1.5
B	MIU-4	MIU-4FT6-02	HBG	−68,243.9	5,401.5	−257.2	3.24	0.79	88.5	61.4 $\pm$ 1.5
B	MIZ-1	MIZ01RA01	HBG	−68,867.7	6,503.7	95.7	6.97	1.98	95.8	71.5 $\pm$ 1.8
B	MIZ-1	MIZ01RA03	HBG	−68,867.7	6,503.7	23.7	6.74	1.96	94.6	73.1 $\pm$ 1.8
B	MIZ-1	MIZ01RA05	HBG	−68,825.1	6,546.3	−69.9	7.03	2.01	95.5	72.1 $\pm$ 1.8
O	Mitake	KA-5Bi	MBG	−63,940.0	350.0	290.0	7.06	2.20	91.2	78.5 $\pm$ 3.9
O	Fukazawa	KA-6Bi	MBG	−60,947.9	6,706.5	290.0	7.02	2.16	91.3	77.3 $\pm$ 3.9
O	Kamado	KA-7Bi	MBG	−65,670.0	12,380.0	268.0	7.09	2.01	89.8	71.4 $\pm$ 3.6
O	Garaishi	KA-8Bi	MBG	−66,730.0	3,535.0	330.0	6.90	2.11	91.1	76.9 $\pm$ 3.8
O	Tsukiyoshi	KA-9Bi	HBG	−69,385.0	5,885.0	179.0	5.96	1.78	93.2	75.2 $\pm$ 3.8
O	Jorinji	KA-10Bi	MBG	−68,827.5	3,162.5	230.0	6.49	1.96	82.0	75.9 $\pm$ 3.8
O	Tokiguchi	KA-11Bi	MBG	−72,025.0	390.0	130.0	6.24	1.94	91.6	78.3 $\pm$ 3.9

<sup>a</sup> Rock facies of the Toki granite includes muscovite-biotite granite (MBG), hornblende-biotite granite (HBG), and biotite granite (BG)

distribution shift in track length, based on comparison with standard fission-track length sample (Fish Canyon Tuff: reheating-free sample).

### Thermochronology: K–Ar dating and fission-track dating

The results of the K–Ar dating and fission-track dating for minerals are listed in Tables 2, 3, and 4. Hornblende K–Ar ages are about  $74.3 \pm 3.7$  Ma (Fig. 3). Biotite K–Ar ages

range from  $78.5 \pm 3.9$  to  $59.7 \pm 1.5$  Ma, with a distribution of approximately 20 Ma (Fig. 3). The zircon fission-track ages range from  $75.6 \pm 3.3$  to  $52.8 \pm 2.6$  Ma, with a scatter of 23 Ma (Fig. 3). Characterization of zircon fission-track length measurements gives almost the same results for nine samples, which show normal frequency distribution ranging from 5 to 12  $\mu\text{m}$  (Table 5; Fig. 4). Mean fission-track length clusters range from 10 to 11  $\mu\text{m}$  with a single frequency peak (Fig. 4). This result indicates that the ages do not represent rejuvenation by massive reheating during the cooling process.

**Table 4** Zircon fission-track dating results from the Toki Granite

Sample description Borehole (B)/ outcrop (O)	Rock facies <sup>a</sup>	Location and elevation		N***		Spontaneous		Induced		P (x <sup>2</sup> )		Dosimeter		r	U (ppm)	Age (Ma) ± 1σ
		X (northing)	Y (easting)	Elevation (m)	ρ <sub>s</sub> (10 <sup>-6</sup> cm <sup>-2</sup> )	N <sub>s</sub> (10 <sup>-6</sup> cm <sup>-2</sup> )	ρ <sub>i</sub> (10 <sup>-6</sup> cm <sup>-2</sup> )	N <sub>i</sub> (10 <sup>-6</sup> cm <sup>-2</sup> )	ρ <sub>d</sub> (10 <sup>-4</sup> cm <sup>-2</sup> )	N <sub>d</sub> (10 <sup>-4</sup> cm <sup>-2</sup> )						
B DH-2	HBG	-69,125.0	6,437.4	-185.0	30	9.15	3,814	2.20	918	0	8.138	4,167	0.489	260	63.9 ± 2.6	
B DH-2	BG	-69,125.0	6,437.4	-302.1	30	8.95	3,402	2.41	917	10	8.153	4,174	0.644	280	57.2 ± 2.3	
B DH-3	MBG	-64,489.2	4,416.3	77.0	30	7.51	4,764	1.95	1,239	70	8.698	4,453	0.779	210	63.2 ± 2.3	
B DH-3	MBG	-64,489.2	4,416.3	-479.7	30	8.12	4,612	2.00	1,134	0	8.715	4,462	0.698	220	67.0 ± 2.5	
B DH-6	MBG	-66,630.9	978.7	13.3	30	8.78	3,584	1.98	807	0	8.370	2,571	0.332	190	65.1 ± 2.9	
B DH-6	MBG	-66,630.9	978.7	-126.9	30	8.46	3,731	1.87	823	0	8.373	2,572	0.525	180	66.5 ± 2.9	
B DH-6	MBG	-66,630.9	978.7	-473.6	20	9.63	2,657	2.25	621	3	8.377	2,573	0.611	220	62.8 ± 3.1	
B DH-6	MBG	-66,630.9	978.7	50.8	30	11.10	4,826	2.37	1,030	1	8.380	2,574	0.386	230	68.7 ± 2.8	
B DH-8	MBG	-66,002.9	1,871.9	47.3	30	9.23	4,599	1.71	854	0	8.025	2,465	0.407	170	75.6 ± 3.3	
B DH-8	MBG	-66,002.9	1,871.9	-88.2	30	9.25	4,348	1.90	891	3	8.027	2,466	0.479	190	68.6 ± 2.9	
B DH-8	MBG	-66,002.9	1,871.9	-439.6	30	10.70	5,519	2.10	1,082	0	8.029	2,467	0.585	210	71.7 ± 2.9	
B DH-8	MBG	-66,002.9	1,871.9	-610.7	30	8.80	5,115	1.77	1,031	0	8.031	2,467	0.786	180	69.7 ± 2.8	
B DH-8	MBG	-66,002.9	1,871.9	-739.7	30	8.64	5,799	1.77	1,188	17	8.033	2,468	0.735	180	68.6 ± 2.7	
B DH-10	MBG	-63,745.2	10,945.7	196.2	30	7.31	4,482	1.62	996	23	8.612	4,409	0.664	180	73.2 ± 2.9	
B DH-10	MBG	-63,745.2	10,945.7	-256.2	30	6.08	5,401	1.34	1,191	14	8.131	4,163	0.663	160	69.7 ± 2.5	
B DH-11	BG	-67,285.4	7,560.5	-116.7	30	9.79	3,662	2.58	964	11	8.629	4,418	0.526	280	62.0 ± 2.5	
B DH-11	BG	-67,285.4	7,560.5	-411.9	30	9.85	3,221	2.51	822	5	8.646	4,427	0.675	270	64.1 ± 2.7	
B DH-12	MBG	-70,695.4	3,935.0	-246.7	30	9.65	4,158	2.70	1,163	0	8.663	4,436	0.647	290	58.6 ± 2.2	
B DH-13	HBG	-65,324.7	8,625.8	-77.0	30	12.00	3,696	3.31	1,019	0	8.680	4,444	0.636	360	59.5 ± 2.3	
B MIU-1	HBG	-68,280.3	5,217.4	108.6	30	11.00	3,828	2.59	902	9	8.356	2,567	0.657	250	62.1 ± 2.7	
B MIU-1	HBG	-68,280.3	5,217.4	-261.9	30	10.80	4,080	2.48	939	0	8.359	2,568	0.507	240	63.6 ± 2.7	
B MIU-1	BG	-68,280.3	5,217.4	-360.9	30	9.50	4,313	2.35	1,065	1	8.363	2,569	0.410	230	59.3 ± 2.4	
B MIU-1	BG	-68,280.3	5,217.4	-520.1	30	10.20	2,989	2.55	744	0	8.366	2,570	0.414	240	58.9 ± 2.7	
B MIU-4	HBG	-68,292.4	5,353.0	-98.6	30	10.40	4,864	2.71	1,265	1	8.456	2,165	0.645	260	57.0 ± 2.2	
B MIU-4	HBG	-68,268.6	5,376.8	-176.5	30	9.55	4,786	2.52	1,263	10	8.562	2,192	0.555	240	56.9 ± 2.2	
B MIU-4	HBG	-68,243.9	5,401.5	-257.2	28	11.20	3,415	2.85	873	1	8.601	2,202	0.355	270	58.9 ± 2.6	
B MIU-4	HBG	-68,241.2	5,404.2	-266.2	30	9.80	3,519	2.47	887	0	8.496	2,175	0.599	230	59.1 ± 2.6	
B MIU-4	HBG	-68,237.2	5,408.2	-279.3	30	9.89	2,808	2.68	761	2	8.522	2,182	0.720	250	55.1 ± 2.6	
B MIU-4	HBG	-68,271.4	5,374.0	-167.3	30	14.00	4,953	3.45	1,223	2	8.617	2,206	0.422	360	61.1 ± 2.4	
B MIU-4	HBG	-68,259.1	5,386.3	-207.7	30	12.60	5,409	3.43	1,469	5	8.619	2,206	0.376	360	55.6 ± 2.1	
B MIU-4	HBG	-68,231.9	5,413.5	-296.5	30	11.70	3,453	3.25	956	0	8.620	2,207	0.551	340	54.6 ± 2.4	
B MIZ-1	HBG	-68,867.7	6,503.7	98.4	30	9.91	4,628	2.54	1,184	0	8.043	4,118	0.667	300	59.5 ± 2.2	
B MIZ-1	HBG	-68,867.7	6,503.7	28.1	30	8.62	4,381	2.10	1,068	9	8.057	4,125	0.774	250	62.5 ± 2.4	
B MIZ-1	HBG	-68,825.1	6,546.3	-69.9	30	9.09	4,563	2.46	1,237	0	8.072	4,133	0.583	290	56.3 ± 2.1	
B MIZ-1	HBG	-68,867.7	6,503.7	-6.1	30	10.80	3,981	2.90	1,066	4	8.087	4,140	0.739	340	57.1 ± 2.2	

Table 4 continued

Sample description Borehole (B)/ Outcrop (O)	Sample name	Rock facies <sup>a</sup>		Location and elevation		N <sup>**</sup> : Spontaneous		Induced		P (χ <sup>2</sup> ) Dosimeter		r	U (ppm)	Age (Ma) ± 1σ		
		X (northing)	Y (easting)	Elevation (m)	ρ <sub>s</sub> (10 <sup>-6</sup> cm <sup>-2</sup> )	N <sub>s</sub> (10 <sup>-6</sup> cm <sup>-2</sup> )	ρ <sub>i</sub> (10 <sup>-6</sup> cm <sup>-2</sup> )	N <sub>i</sub> (10 <sup>-6</sup> cm <sup>-2</sup> )	ρ <sub>d</sub> (10 <sup>-4</sup> cm <sup>-2</sup> )	N <sub>d</sub> (10 <sup>-4</sup> cm <sup>-2</sup> )						
B MIZ-1	RA08	HBG	-68,867.7	6,503.7	16.5	30	10.40	3,848	2.78	1,026	34	8.102	4,148	0.521	320	57.5 ± 2.3
B MIZ-1	RA09	HBG	-68,867.7	6,503.7	16.5	29	10.40	2,404	2.47	574	47	8.116	4,156	0.696	290	64.3 ± 3.2
O Mitake	FT-9	MBG	-63,940.0	350.0	290.0	30	6.48	5,218	1.52	1,221	0	8.352	2,566	0.674	150	62.5 ± 2.4
O Fukazawa	FT-10	MBG	-60,947.9	6,706.5	290.0	30	7.71	3,578	1.79	829	0	8.342	2,563	0.591	170	63.1 ± 2.8
O Kamado	FT-11	MBG	-65,670.0	12,380.0	268.0	21	13.60	2,337	3.77	648	3	8.245	2,564	0.770	360	52.8 ± 2.6
O Garaishi	FT-12	MBG	-66,730.0	3,535.0	330.0	30	8.19	4,600	1.92	1,081	0	8.384	2,576	0.628	180	62.5 ± 2.5
O Tsukiyoshi	FT-13	HBG	-69,385.0	5,885.0	179.0	30	8.63	3,799	2.25	992	2	8.387	2,577	0.588	220	56.3 ± 2.3
O Jorinji	FT-14	MBG	-68,827.5	3,162.5	230.0	30	8.73	3,371	1.93	745	0	8.338	2,561	0.620	190	66.1 ± 3.0
O Tokiguchi	FT-15	MBG	-72,025.0	390.0	130.0	30	7.67	4,280	1.73	963	0	8.349	2,565	0.564	170	65.0 ± 2.7

Analyses were obtained by the external detector method using internal mineral surfaces and a geometry factor of 0.5 (EDI: Gleadow 1981)

N<sup>\*\*</sup> denotes the number of grains. ρ<sub>s</sub> is the spontaneous track density (tracks/cm<sup>2</sup>) in the grain, and N<sub>s</sub> stands for the number of spontaneous tracks. ρ<sub>i</sub> and N<sub>i</sub> are the induced track density (tracks/cm<sup>2</sup>) and number, respectively, in the external detector (tracks/cm<sup>2</sup>). ρ<sub>d</sub> is the track density (tracks/cm<sup>2</sup>), and N<sub>d</sub> stands for the number of tracks in the dosimeter glass. P(χ<sup>2</sup>) is the probability of obtaining the χ<sup>2</sup>-value for n degrees of freedom. r is the correlation coefficient between ρ<sub>s</sub> and ρ<sub>i</sub>. Details of experimental conditions and calibration factors are described by Iwano and Danhara (1997) and Danhara et al. (2003)

<sup>a</sup> Rock facies of the Toki granite includes muscovite-biotite granite (MBG), hornblende-biotite granite (HBG), and biotite granite (BG)

The mineral age will represent the time at which a mineral cooled down to its closure temperature, if the Toki granitic pluton was emplaced as a one pulse or if the emplacement duration is much shorter than the cooling duration in the case of multiple pulse intrusion. The Toki granite shows three rock facies with variations of mineral assemblage among them, without accompanying chilled margin. They have neither mingling texture nor non-equilibrium mineral assemblage. Plagioclase has no dusty zone, indicating the absence of magma mixing. These lines of evidence suggest the single pulse intrusion of the Toki granite in terms of petrography. The dating of the Toki granite using monazite CHIME and whole-rock Rb–Sr method gives 72.3 ± 3.9 Ma (Suzuki and Adachi 1998) and 68.3 ± 1.8 Ma (Shibata and Ishihara 1979), respectively, which will represent the emplacement age (Albarède 2003). The whole-rock Rb–Sr age determined by 14 isotopic data collected through three rock facies (4 samples of MBG, 5 samples of HBG, and 5 samples of BG) is 71.04 ± 1.44 Ma (future work: A Sr isotope variation in the Toki Granite will be the subject of a separate study), which is consistent with the result of Shibata and Ishihara (1979). Hornblende K–Ar age represents a timing with closure temperature of 510 ± 25°C, which are about 74.3 ± 3.7 Ma (Table 2). These dating results cluster in a range of about 4 million years, which implies that the total emplacement duration is either shorter than, or equal to, 4 million years. The duration from the hornblende K–Ar age to the youngest age in zircon fission-track dating is about 22 million years (Fig. 3), which represents cooling duration from 510 ± 25 to 240 ± 50°C. The duration from the hornblende K–Ar age to the youngest age in apatite fission-track is about 42 million years (future work: spatial variation of apatite fission-track ages will be the subject of a separate study), which corresponds to the cooling duration from 510 ± 25 to 120 ± 20°C. These petrographical observations and chronological results indicate that the total emplacement duration of the Toki granite is much shorter than the total cooling duration. Therefore, since the age of a mineral represents the age when the Toki granite cooled down to the closure temperature of the mineral, the older age represents more rapid cooling than the younger age. The spatial cooling history inside the granite can be clarified by a combination of biotite K–Ar and zircon fission-track ages (Tables 3, 4). Hornblende K–Ar age was excluded from consideration, because of their limited distribution to only one borehole (N = 2) (Table 2). The results for the biotite K–Ar and zircon fission-track dating exhibit distribution in excess of the two-sigma level for each mineral age, indicating differences in cooling rate inside the granite pluton (Fig. 3). Age data collected from borehole and outcrop samples were interpolated and



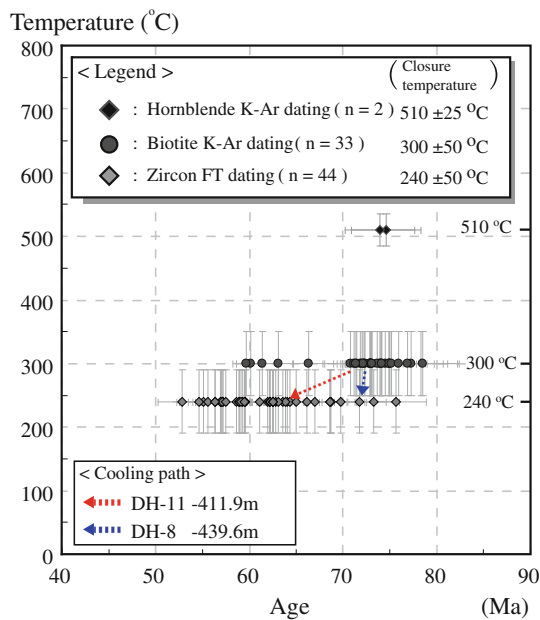


**Fig. 3** Age distribution against closure temperatures. Closure temperatures of the three minerals are from Dodson and McClelland-Brown (1985) and Hurford (1986): hornblende, K–Ar 510 ± 25°C; biotite, K–Ar 300 ± 50°C; zircon, Fission-track 240 ± 50°C. Red and blue dash arrows denote the sub-solidus temperature–time path of DH-11 –411.9 m elevation (central region of the granite body) and DH-8 –439.6 m elevation (northwest margin), respectively

converted to 3-D data for visualization using the software Rock Works 14®.

MBG possesses biotite K–Ar age ranging from 78.5 ± 3.9 to 71.4 ± 3.9 Ma (N = 16) and zircon fission-track age from 75.6 ± 3.3 to 52.8 ± 2.6 Ma (N = 20) (Tables 3, 4). HBG shows the biotite age varying from 75.2 ± 3.8 to 59.7 ± 1.5 Ma (N = 12) and the zircon age

from 64.3 ± 3.2 to 54.6 ± 2.4 Ma (N = 19). BG presents the biotite age ranging from 74.9 ± 3.7 to 66.3 ± 1.7 Ma (N = 5) and the zircon age from 64.1 ± 2.7 to 57.2 ± 2.3 Ma (N = 5). The oldest ages in both datings are recognized in MBG. Figure 5A and B show the contoured spatial distribution of biotite K–Ar ages and zircon fission-track ages, respectively, on fence and block diagrams. Vertical elevations given in the text are with respect to the mean sea level, not the depth from the topographic surface, i.e., positive/negative value denotes upper/lower region with respect to the mean sea level, respectively. This allows a comparison of the age data in terms of the vertical coordinate (elevation). The distribution of biotite K–Ar ages has the same tendency as that of the zircon fission-track ages. The youngest ages (warm colors) are found in the deeper regions of the MIU sites, and the oldest ages (cold colors) are distributed at the northwest upper margin of the pluton (Fig. 5A, B). The biotite K–Ar dating gives ages of 61.4 ± 1.5 Ma in the central deeper region (–257.2 m elevation of MIU-4) and of 72.9 ± 1.8 Ma at the northwest upper margin (47.3 m elevation of DH-8) (Table 3). Table 4 shows the zircon fission-track ages of 58.9 ± 2.7 Ma in the central deeper region (–520.1 m elevation of MIU-1) and of 68.7 ± 2.8 Ma at the northwest upper margin (50.8 m elevation of DH-6). The zircon fission-track age indicates that the Toki granite effectively cooled from the roof and the northwest margin from 75 to 65 Ma (Fig. 5B). Then the northeast margin cooled down in the period from 65 to 61 Ma (Fig. 5B) followed by the southern and central regions (boreholes MIU-1 to –4) from 61 to 55 Ma (Fig. 5B). These data show that the cooling started from the roof and the northwest margin of the Toki granite and then extended to the northeast and further to the central and southern regions.

**Table 5** Characterization of zircon fission-track length measurements

Sample description		Age (Ma) ± 1σ	Track number	Fission-track length					
Borehole (B)/standard (S)	Sample name			Mean (μm)	Min. (μm)	Max. (μm)	Standard deviation	Standard error	
B	DH-2	RA01	63.9 ± 2.6	50	10.54	7.59	11.65	0.62	0.09
B	DH-2	RA03	57.2 ± 2.3	50	10.54	8.24	11.83	0.83	0.12
B	DH-10	DH10RA	69.7 ± 2.5	50	10.43	5.12	11.83	1.16	0.16
B	MIZ-1	RA01	59.5 ± 2.2	50	10.27	5.30	11.89	1.14	0.16
B	MIZ-1	RA03	62.5 ± 2.4	50	10.47	8.35	11.88	0.66	0.09
B	MIZ-1	RA05	56.3 ± 2.1	50	10.56	6.88	11.97	0.88	0.12
B	MIZ-1	RA07	57.1 ± 2.2	50	10.40	6.34	11.96	0.88	0.12
B	MIZ-1	RA08	57.5 ± 2.3	50	10.06	5.68	11.66	1.32	0.19
B	MIZ-1	RA09	64.3 ± 3.2	50	10.26	7.58	11.86	0.91	0.13
S	Fish Canyon Tuff		–	50	10.66	9.35	12.73	0.67	0.10

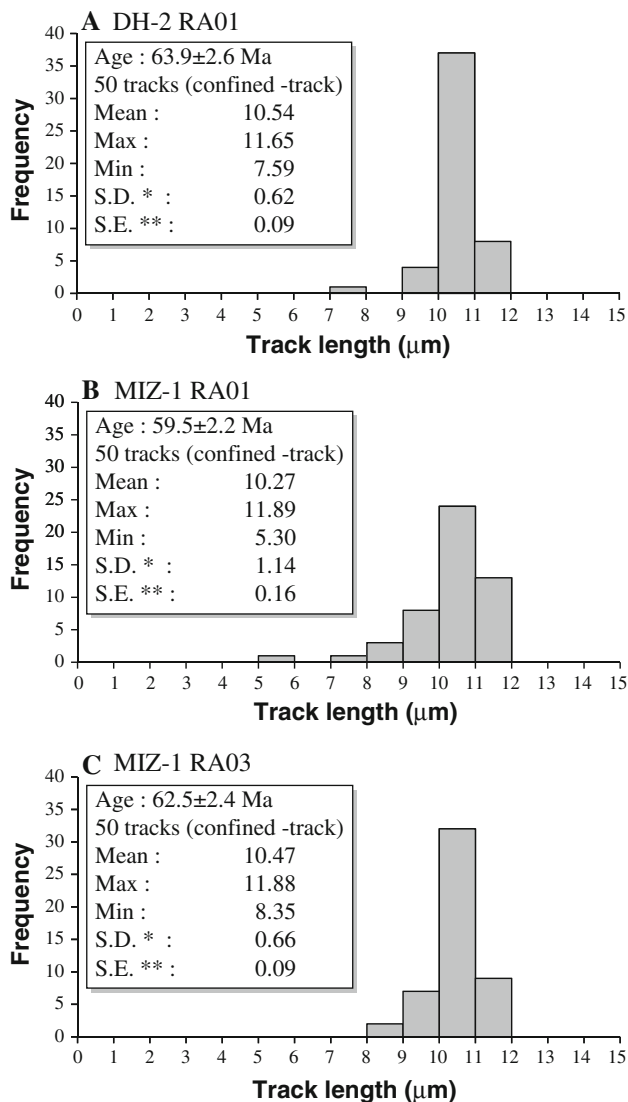


**Fig. 4** Frequency distribution of zircon fission-track length in three samples (**a** DH-2 RA01, **b** MIZ-1 RA01, and **c** MIZ-1 RA03) collected from the Toki granite (\*S.D. standard deviation, \*\*S.E. standard error)

## Discussion

### Duration of cooling from biotite K–Ar closure temperature to zircon fission-track closure temperature

“Sub-solidus temperature–time path” at the particular position inside the Toki granite could be identified by comparing biotite K–Ar age and zircon fission-track age at any particular position (Fig. 3). The gradient of temperature–time path depends on the position inside the granite, as the two representative cooling paths are schematically shown in Fig. 3: DH-11 (−411.9 m elevation at the central region of the granite body) and DH-8 (−439.6 m elevation at the northwest margin). Figure 6A shows a more detailed temperature–time relationship between biotite K–Ar and

zircon fission-track ages in the two samples. The difference between the two ages at one particular position (or two positions within 5 m) inside the granite indicates the cooling duration in which the granite cooled from biotite K–Ar closure temperature ( $300 \pm 50^\circ\text{C}$ ) to zircon fission-track closure temperature ( $240 \pm 50^\circ\text{C}$ ). This cooling duration of the northwest margin of the body (1.3 million years of DH-8) is shorter than that of the central region (8.2 million years of DH-11) (Fig. 6a). Figure 6b shows the contoured spatial distribution of the cooling duration between two closure temperatures on fence diagram, which was colored as a three-dimensional pattern using the software Rock Works 14® based on 33 data (Tables 3, 4). Long durations (warm colors) are found at southern to central region, and short durations (cold colors) are distributed at the northwest and northeast upper margin of the pluton. The cooling duration between two closure temperatures gives about 14.7 million years in the central deeper region (−520.1 m elevation of MIU-1) and of about 3.2 million years at the northwest upper margin (88.2 m elevation of DH-8). The distribution of cooling duration between two closure temperatures (Fig. 6b) has a pattern, consistent with that of cooling pattern based on “multi-sampling thermochronology” (Fig. 5A, B). Thus, the region with relatively early cooling (older ages) corresponds to that of the rapid rate of cooling from biotite K–Ar closure to zircon fission-track closure temperatures, and the region with relatively later cooling (younger ages) also corresponds to that of the slower cooling rate. Assuming simply that temperature difference between biotite K–Ar and zircon fission-track closure is  $60^\circ\text{C}$ , the cooling rate from 300 to  $240^\circ\text{C}$  at the central deeper region is about  $4.1^\circ\text{C/m.y.}$  (−520.1 m elevation of MIU-1) and that of northwest upper margin is  $18.8^\circ\text{C/m.y.}$  (88.2 m elevation of DH-8).

### Factors controlling the cooling process

Figure 7 shows the contoured spatial distribution of the ASI values on the fence diagram based on 483 analyses of samples collected from boreholes in the Toki granite. Original data are taken from Yuguchi et al. (2010). The ASI values increase systematically from the roof downward. The minimum ASI value (in purple) occurs in the lower central region and larger values (warm colors) are distributed near the upper northwest margin (Fig. 7).

Yuguchi et al. (2010) discussed that the intrusion/emplacement process of the Toki granitic pluton probably includes the assimilation of crustal country rocks into the granitic magma. The ASI values can be an index of the assimilation of the older sedimentary rock into the granitic magma (Pitcher 1997). Yuguchi et al. (2010) also described (1) the comparison of ASI between the Toki granite

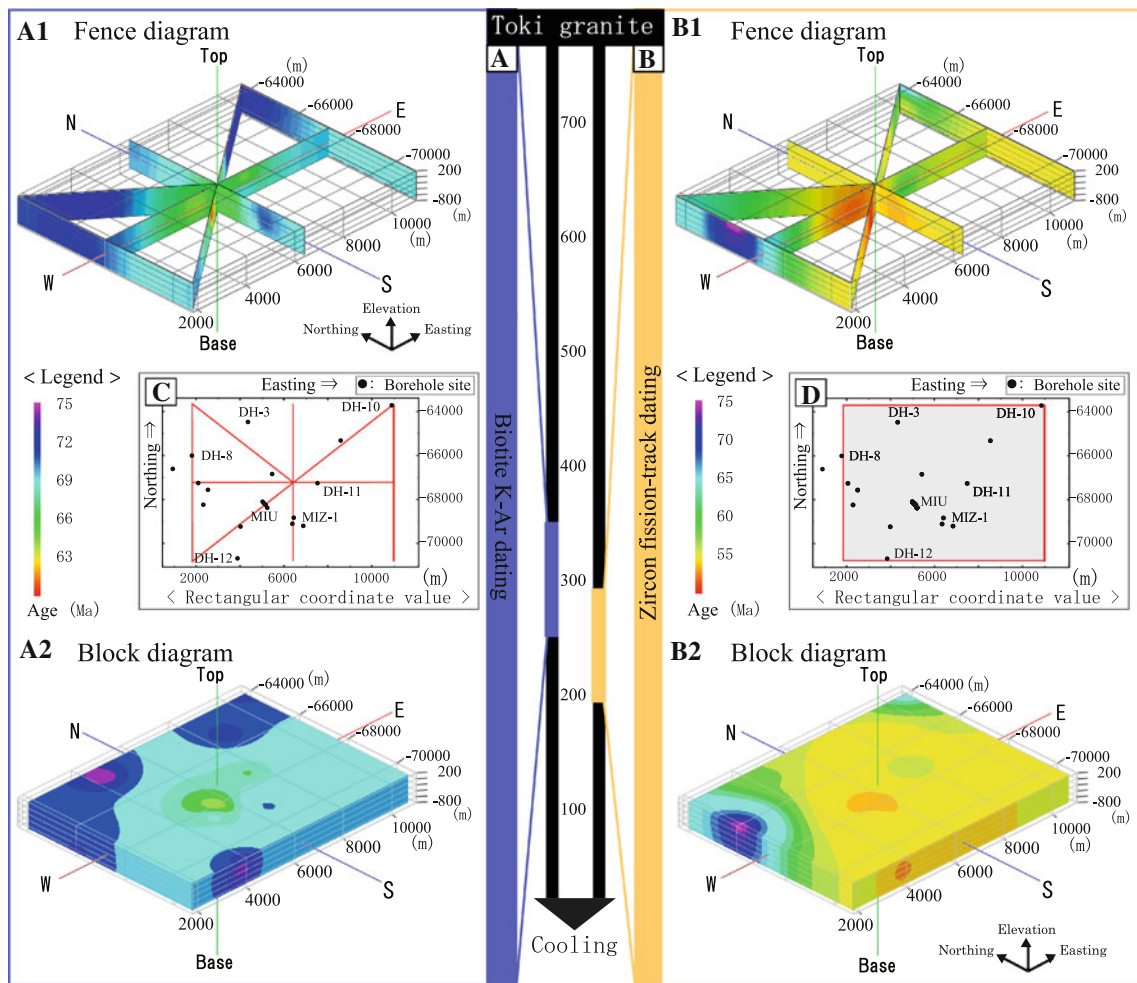


**Fig. 5** Contoured spatial distribution of biotite K–Ar ages (A) and zircon fission-track ages (B) in the Toki granite. The fence diagrams (A1 and B1) along the lines on the borehole site map (C) and the block diagrams (A2 and B2) inside the enclosed area in the borehole site map (D) were constructed based on 33 biotite K–Ar age dates and 44

zircon Ft age dates. To make these diagrams, the data were interpolated and converted to 3-D data for visualizing of the subsurface geological evidence using Rock Works 14. Northing and easting in the borehole map are expressed based on the rectangular coordinate system with the origin of 137°10'00"E/36°00'00"N

and the country sedimentary rocks of the Mino Terrane and (2) the rare occurrence of the xenolith in the granite, which implies either that the xenolith was completely assimilated by the granitic magma or that the melt extracted from partially molten country rock was assimilated into the granitic magma. The country rock of the Toki granite is the Nohi Rhyolite on the east of the body and the sedimentary rocks of the Mino Terrane on the west. Assimilation of the sedimentary rocks of the Mino Terrane can yield the larger ASI than that of the Nohi Rhyolite. In fact, ASI value of the Nohi Rhyolite is almost equal to that of HBG and BG in the Toki granite (Yuguchi et al. 2010; Sonehara and Harayama 2007). Larger ASI values are distributed near the northwest margin in contact with the metasedimentary rocks (hornfels) of the Mino Terrane. Thus, geology around the Toki granite and ASI distribution inside the granite imply that the assimilation by the Toki granitic magma operated

during in situ emplacement process, but not during magma ascent process before the emplacement.

Both biotite K–Ar dating and zircon fission-track dating show the same cooling pattern. The older age represents earlier and more rapid cooling, because mineral age is equivalent to the time at which the Toki granite cooled down to the closure temperature. Thus, the Toki granite effectively cooled down from the roof and also from the northwest margin at temperatures between  $300 \pm 50$  and  $240 \pm 50^\circ\text{C}$ . There is a strong correlation between ASI (Fig. 7) and the cooling behavior of the pluton during this temperature stage (Figs. 5, 6). Large ASI values correspond to earlier and more rapid cooling after intrusion and smaller values to slower cooling. This consistency between cooling rate and ASI value strongly suggests that the intrusion/emplacement process of the Toki granitic magma was affected by assimilation. Incorporation of country

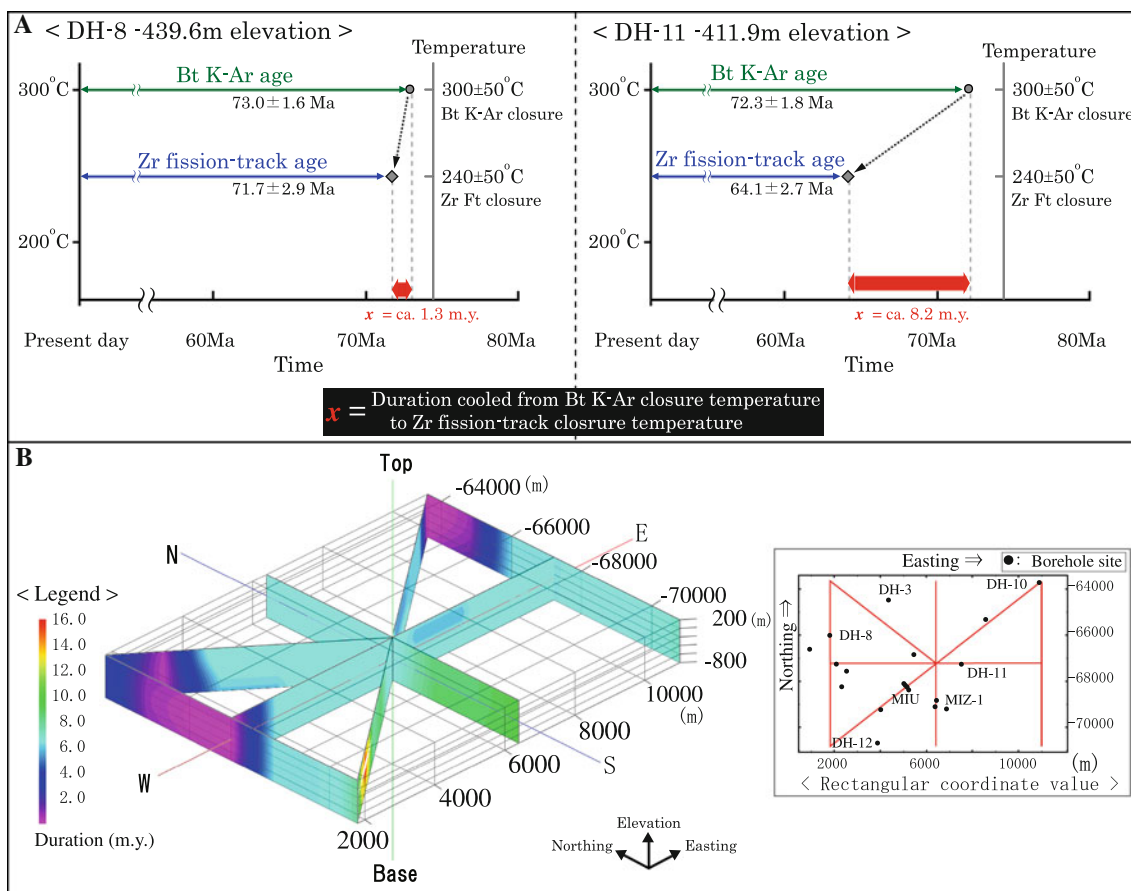


**Fig. 6** Duration of cooling from biotite K–Ar closure temperature ( $300 \pm 50^\circ\text{C}$ ) to zircon fission-track closure ( $240 \pm 50^\circ\text{C}$ ). **a** Example of the duration  $x$  (1.3 m.y.) at “DH-8 –439.6 m elevation (northwest margin of the body; left)” and that (8.2 m.y.) at “DH-11 –

411.9 m elevation (central region; right).” **b** Contoured spatial distribution of the duration of cooling from biotite K–Ar closure temperature to zircon fission-track closure on a fence diagram (using Rock Works 14), based on 33 borehole and outcrop datum

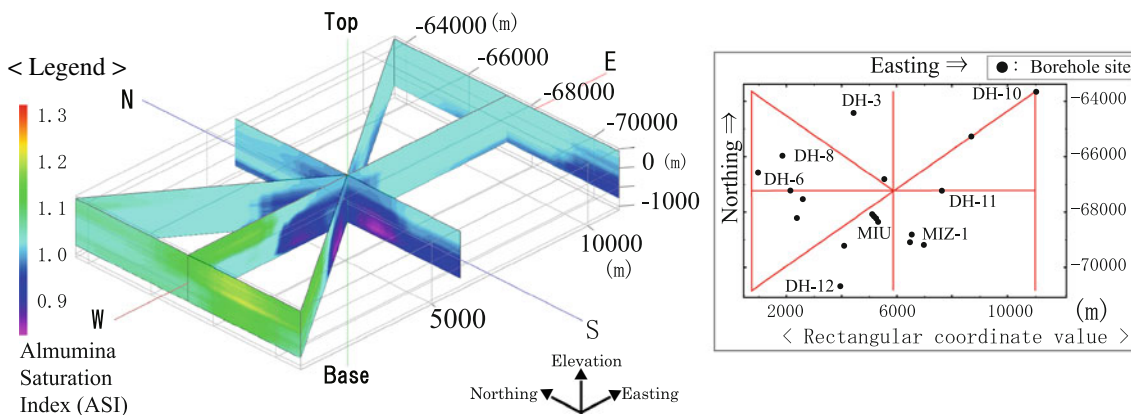


**Fig. 7** Contoured spatial distribution of ASI values on a fence diagram (using Rock Works 14), based on 483 borehole samples in the Toki granite. Original data ( $N = 483$ ) on the bulk chemical composition are described in Yuguchi et al. (2010)

rocks into magma requires a lot of thermal energy to dissolve the country rocks (Glazner 2007). That is, the Toki granite was effectively cooled from the peraluminous regions where assimilation of country rock was most extensive.

Contributions to thermal modeling

Thermal models of granitic cooling have been often discussed numerically (e.g., Okudaira 1996; Scaillet et al. 1996; Annen et al. 2001; Annen 2009, 2011), which would

be useful procedure to acquire the “temporal variation” of cooling pattern of the granitic pluton. Okudaira (1996) described the thermal history of the granitic pluton and its surrounding rocks in the vertical direction by using a 1-D heat transport model. Scaillet et al. (1996) and Annen (2009) presented the 2-D steady-state thermal model of the crust on the cross-section to evaluate the cooling history after the intrusion. The result of numerical model depends largely on a shape of the plutonic body (e.g., thickness and width) and values of parameters (e.g., density, heat capacity, thermal conductivity and latent heat of the plutonic and country rocks, and the heat production rate by radiometric decay in the crust) and hence includes some uncertainty inevitably. In the case of the Toki granite, the boundary condition cannot be well defined, because the shape of the body is not well known. It is very difficult in such a case to reveal three-dimensional cooling pattern precisely based on the 3-D numerical model. At this point, multi-sampling thermochronology has a benefit as a practical method to reveal three-dimensional cooling pattern such a granitic body. However, we have to note that the cooling pattern clarified in this study is a “snapshot” of the moment when the Toki granite cooled down to the closure temperature of target mineral.

Memeti et al. (2010) discussed magma chamber evolution of the Tuolumne batholith, Sierra Nevada, California, by a combination of thermochronology (U–Pb zircon age and  $^{40}\text{Ar}/^{39}\text{Ar}$ ) and 2-D finite difference thermal modeling. Thermochronology shows a “moment cooling pattern” and thermal model shows a “temporal variation of cooling pattern.” The combination of the two can give more information for thermal history of the granite body than either one. Our study concludes that the multi-sampling thermochronology provides three-dimensional cooling pattern of the granitic pluton which is correlated with chemistry (ASI value). Therefore, if both chronological data and chemistry can be incorporated into numerical model as parameters, it may yield practical thermal model to understand more accurately the temporal change of cooling pattern, which remains as a future study.

## Conclusions

Samples collected from 11 boreholes and seven outcrops in the Toki granite exhibit spatial variations in mineral ages inside the zoned granitic pluton. The result of “multi-sampling thermochronology” based on multiple mineral dating with different closure temperatures therefore represents a good indicator of the cooling behavior (cooling pattern and cooling rate) in a granitic pluton. The biotite K–Ar dating and zircon fission-track dating show similar patterns in the Toki granite, giving the central deeper region

of the pluton has the youngest ages and the northwest upper margin shows the oldest ages. The region with the older ages corresponds to that of the rapid rate of cooling from biotite K–Ar closure ( $300 \pm 50^\circ\text{C}$ ) to zircon fission-track closure ( $240 \pm 50^\circ\text{C}$ ), and the region with the younger ages also corresponds to that of the slower cooling rate. Thus, the Toki granite cooled from the roof and the northwest margin of the Toki granite, and then cooling extended to the northeast and further to the central and southern regions. The ASI value becomes larger toward the margin of the Toki granite. There is a strong correlation between the cooling rate and ASI value: large ASI corresponds to more rapid cooling rate and vice versa. A linkage between the cooling pattern and chemistry is interpreted as that the Toki granite was effectively cooled from the peraluminous regions where assimilation of country rock was most extensive. Thus, the intrusion/emplacement process of the Toki granitic magma was affected by the assimilation. This study combining thermochronology and petrographical methods can delineate a quantitative cooling pattern of a granite at the temperature condition between biotite K–Ar closure and zircon fission-track closure, providing a vital piece of information to reveal the record of the post-kinematic granitic pluton during the period from the intrusion stage, through the sub-solidus stage to the present day.

**Acknowledgments** The technical comments and English review by Mr. G. McCrank, an ex-JAEA International Fellow, are appreciated. Constructive reviews by Drs. J. Žák, L. Caricchi, and J. Blundy (associated editor) were very helpful in revising the manuscript. The authors also thank researchers from the Mizunami Underground Research Laboratory, Japan Atomic Energy Agency, for their discussion and suggestion.

## References

- Albarède F (2003) *Geochemistry: an introduction*. Cambridge University Press, UK, p 248
- Annen C (2009) From plutons to magma chambers: thermal constraints on the accumulation of eruptible silicic magma in the upper crust. *Earth Planet Sci Lett* 284:409–416
- Annen C (2011) Implications of incremental emplacement of magma bodies for magma differentiation, thermal aureole dimensions and plutonism-volcanism relationships. *Tectonophysics* 500:3–10. doi:10.1016/j.tecto.2009.04.010
- Annen C, Lénat J-F, Privost A (2001) The long-term growth of volcanic edifices: numerical modelling of the role of dyke intrusion and lava-flow emplacement. *J Vol Geotherm Res* 105:263–289
- Asia Air Survey (1997) Geological survey on regional scale in Tono Area. JNC TJ 2000-027 (in Japanese with English Abstract)
- Bando M, Bignall G, Sekine K, Tsuchiya N (2003) Petrography and uplift history of the Quaternary Takidani Granodiorite: could it have hosted a supercritical (HDR) geothermal reservoir? *J Volcanol Geotherm Res* 120:215–234
- Cox A, Dalrymple GB (1967) Statistical analysis of geomagnetic reversal data and the precision of potassium-argon dating. *J Geophys Res* 72:2603–2614

- Dalrymple GB, Lanphere MA (1969) Potassium-argon dating; principles techniques, and applications to geochronology. W. H. Freeman and Co., San Francisco, pp 258
- Dalrymple GB, Grove M, Lovra OM, Harrison TM, Hulen JB, Lanphere MA (1999) Age and thermal history of the Geysers plutonic complex (felsite unit), Geysers geothermal field, California: a  $^{40}\text{Ar}/^{39}\text{Ar}$  and U-Pb study. *Earth Planet Sci Lett* 173:285–298
- Danhara T, Iwano H (1983) The zeta age calibration of fission-track dating. *Isotope Geosci* 1:285–317
- Danhara T, Iwano H, Yoshioka T, Tsuruta T (2003) Zeta calibration values for fission track dating with a diallyl phthalate detector. *J Geol Soc Jpn* 109:665–668 (in Japanese with English abstract)
- Dodson H, McClelland-Brown E (1985) Isotopic and paleomagnetic evidence for rates of cooling, uplift and erosion. In: Snelling J (ed) Geological society of London memories 10, Oxford, London, pp 315–325
- Eby GN, Roden-Tice M, Kyueger HL, Ewing W, Faxon EH, Woolley AR (1995) Geochronology and cooling history of the northern part of the Chilwa Alkaline Province, Malawi. *J Afr Earth Sci* 20:275–288
- Fujii Y (2000) Fracture analysis of the Toki Granite in the Tono district, central Japan. *J Geol Soc Japan* 106:249–263 (in Japanese with English abstract)
- Glazner AF (2007) Thermal limitations on incorporation of wall rock into magma. *Geology* 35:319–322
- Gleadow AJW (1981) Fission-track dating methods: what are the real alternatives? *Nucl Tracks Methods Instrum Appl* 5:3–14
- Gleadow AJW, Lovering JF (1977) Geometry factor for external detectors in fission track dating. *Nucl Track Detect* 1:99–106
- Gleadow AJW, Hurford AJ, Quaipe RD (1976) Fission track dating of zircon: improved etching techniques. *Earth Planet Sci Lett* 33:273–276
- Harayama S (1992) Youngest exposed granitoid pluton on Earth: cooling and rapid uplift of the Pliocene—quaternary Takidani Granodiorite in the Japan Alps, central Japan. *Geology* 20:657–660
- Harayama S (1994) Cooling history of the youngest exposed pluton in the world—the Plio-Pleistocene Takidani Granodiorite (Japan Alps, central Japan). *Mem Geol Soc Japan* 43:87–97 (in Japanese with English abstract)
- Hurford AJ (1986) Cooling and uplift patterns in the Lepontine Alps South Central Switzerland and an age of vertical movement on the Insubric fault line. *Contrib Mineral Petrol* 92:413–427
- Hurford AJ (1990a) Standardization of fission track dating calibration: recommendation by the fission track working group of the I.U.G.S. Subcommittee of geochronology. *Chem Geol* 80:171–178
- Hurford AJ (1990b) International union of geological science subcommission on geochronology recommendation for the standardization of fission track dating calibration and data reporting. *Nucl Track Radiat Meas* 17:233–236
- Hurford AJ, Green PF (1983) The zeta age calibration of fission-track dating. *Isotope Geosci* 1:285–317
- Ishihara S (2003) Chemical contrast of the Late Cretaceous granitoids of the Sanyo and Ryoke Belts, Southwest Japan: Okayama-Kagawa Transect. *Bull Geol Surv Japan* 54:95–116
- Ishihara S, Chappell B (2007) Chemical compositions of the late Cretaceous Ryoke granitoids of the Chubu District, central Japan—Revisited. *Bull Geol Surv Japan* 58:323–350
- Itoigawa J (1974) Geology of the Mizunami district, central Japan. *Bull Mizunami Fossil Museum* 1:9–42 (in Japanese)
- Itoigawa J (1980) Geology of the Mizunami district, central Japan. *Monogr Mizunami Fossil Museum* 1:1–50 (in Japanese)
- Iwano H, Danhara T (1997) Zeta calibrations of fission-track dating system using high-resolution monitor and comparison of reported zeta values. *Fission Track News Lett* 10:11–20 (in Japanese with English abstract)
- Japan Nuclear Cycle Development Institute (2000) Regional hydrogeological study project result from 1992–1999. JNC technical report, JNC TN7400 2003-007, Tono Geoscience Center, pp 86
- Japan Nuclear Cycle Development Institute (2002) Master plan of the Mizunami underground research laboratory project. JNC technical report, JNC TN7410 2003-001, Tono Geoscience Center, pp 47
- Memeti V, Paterson S, Matzel J, Mudil R, Okaya D (2010) Magmatic lobes as “snapshots” of magma chamber growth and evolution in large, composite batholiths: an example from the Tuolumne intrusion, Sierra Nevada, California. *Geol Soc Am Bull* 24:1912–1931
- Oikawa T, Umeda K, Kanazawa S, Matsuzaki T (2006) Unusual cooling of the Middle Miocene Ichifusayama Granodiorite, Kyushu, Japan. *J Miner Petrol Sci* 101:23–28
- Okudaira T (1996) Thermal evolution of the Ryoke metamorphic belt, southwestern Japan: tectonic and numerical modeling. *Island Arc* 5:373–385
- Ota K, Amano K, Suyama Y, Saegusa H (1999) 3D geological modelling in regional hydrogeological study in the Tono Area. *JNC Tech Rev* 4:101–110
- Pitcher WS (1997) The nature and origin of granite, 2nd edn. Chapman and Hall, London
- Sano H, Yamagata T, Horibo K (1992) Tectonostratigraphy of Mino terrane: Jurassic accretionary complex of southwest Japan. *Palaeogeogr Palaeoclimatol Palaeoecol* 96:41–57
- Scaillet S, Cuney M, Carlier de Veslud C, Cheilletz A, Royer JJ (1996) Cooling pattern and mineralization history of the Saint Sylvestre and western Marche Leucogranite pluton, French Massif Central: II. Thermal modelling and implications for the mechanisms of uranium mineralization. *Geochim Cosmochim Acta* 60:4673–4688
- Shibata K, Ishihara S (1979) Rb-Sr whole-rock and K-Ar mineral ages of granitic rocks in Japan. *Geochem J* 13:113–119
- Sonehara T, Harayama S (2007) Petrology of the Nohi Rhyolite and its related granitoids: a late cretaceous large silicic igneous field in central Japan. *J Volcanol Geotherm Res* 167:57–80
- Steiger RH, Jäger E (1977) Subcommittee on geochronology: convention on the use of decay constants in geo- and cosmochronology. *Earth Planet Sci Lett* 36:359–362
- Suzuki K, Adachi M (1998) Denudation history of the high T/P Ryoke metamorphic belt, southwest Japan: constraints from CHIME monazite ages of gneisses and granitoids. *J Metamor Geol* 16:27–37
- Suzuki K, Nakazaki M, Adachi M (1998) An  $85 \pm 5$  Ma CHIME age for the Agigawa welded tuff sheet in the oldest volcanic sequence of the Nohi Rhyolite, central Japan. *J Earth Planet Sci* 45:17–27
- Tsuchiya N, Fujino K (2000) Evaluation of cooling history of the quaternary Takidani pluton using thermoluminescence technique. *Proceedings of World Geothermal Congress 2000*, pp 3939–3944
- Umeda K, Komatsu R, Tanase A, Yusa Y (2001) Cooling history of the Takahama Granitic Rocks, Shikoku, Ryoke Belt, Southwest Japan, with special reference to the thermal effect of the Neogene intrusive rocks. *Jpn Mag Miner Petrol Sci* 30:17–27 (in Japanese with English abstract)
- Yamada N, Wakita K, Hiroshima T, Komazawa T (1990) Geology of the Iida district. With Geological Sheet Map at 1:200,000. Geological Survey of Japan (in Japanese with English abstract)
- Yamashita N, Kasuno Y, Itoigawa J (1988) Japanese geology 5, Chubu district II. Kyoritsu shuppan, Tokyo (in Japanese)
- Yuguchi T, Tsuruta T, Nishiyama T (2010) Zoning of rock facies and chemical composition in the Toki granitic body, Central Japan.

- Jpn Mag Miner Petrol Sci 39:50–70 (in Japanese with English abstract)
- Yuhara M, Kagami H (1995) Cooling history of the Katsuma quartz diorite in the Ina district of the Ryoke belt, Southwest Japan Arc. J Geol Soc Jpn 101:434–442
- Zhao Z, Zheng Y, Wei C, Gong B (2004) Temporal relationship between granite cooling and hydrothermal uranium mineralization at Dalongshan in China: a combined radiometric and oxygen isotopic study. Ore Geol Rev 25:221–236